PAPER

Check for updates

Bacterial cellulose-poly(acrylic acid-*co*-N,N'-methylene-bis-acrylamide) interpenetrated networks for the controlled release of fertilizers†

Anamaria Zaharia,‡[a] Anita-Laura Radu,‡[a] Stela Iancu,[a] Ana-Mihaela Florea,[a] Teodor Sandu,[a] Iulian Minca,[a] Victor Fruth-Oprisan, [b] Mircea Teodorescu,[c] Andrei Sarbu [ID] *[a] and Tanta-Verona Iordache [ID] *[a]

In this study, composite hydrogels with interpenetrated polymer networks (IPNs), based on bacterial cellulose (BC) and poly(acrylic acid-*co*-N,N'-methylene-bis-acrylamide) (PAA), were synthesized by radical polymerization and characterized herein for the first time. Liquid fertilizer (LF) formulations, containing potassium, phosphorus, ammonium oxides and micronutrients, were encapsulated directly into the IPNs of the composite hydrogels during synthesis. Thermal analyses and scanning electron microscopy of control and composite xerogels highlighted the formation of IPNs between BC and PAA. Swelling determinations confirmed the influence of the crosslinker and of the liquid fertilizer concentration upon the density of the IPNs. Further rheology studies and release profiles indicated how the presence of BC and the increase of the crosslinking density of IPNs improved the mechanical strength and the release profile of LF for the innovative composite BC-PAA hydrogels. Results regarding the fertilizer release indicated that the presence of the BC led to a more controlled liberation of the fertilizer proving that this new formulation is potentially viable for application in agricultural practices.

1 Introduction

Hydrogels are hydrophilic polymers which can absorb and retain significant amounts of water or aqueous solutions.[1] In 1960, Wichterle and Lim first synthesized a hydrogel based on poly(2-hydroxyethyl methacrylate) with potential for biomedical applications.[2] The water absorption and retention properties of hydrogels made possible their use in various biomedical, pharmaceutical and technological fields, with applications such as controlled release systems, encapsulation of cells, tissue repair,[3] electrochemical capacitors[4] and sensors.[5] One of the most important fields where these controlled release systems have found their use is agriculture.[6–8] Thus, controlling the release behaviour in the ground, of either water alone (as water reservoirs) or of various bioactive substances such as fertilizers or pesticide solutions[7,8] is an important step. Plus, delivery systems with controlled release features are generally more efficient and sustainable than the conventional agrochemical formulations, because the excessive treatment of soils is avoided and the equilibrated feed of crops with the active ingredients is maintained.[9,10] For agricultural applications, the most important characteristics of hydrogels are related to biodegradability and high swelling capacities (super-absorbency).[11] One way to optimize these two characteristics is combining synthetic polymers (petrochemical based) with natural polymers (*e.g.* polysaccharide and polypeptide based).[12] For instance, Sannino and co-workers developed biodegradable and biocompatible microporous cellulose-based superabsorbent hydrogels for personal care applications using vegetal cellulose derivatives chemically crosslinked with divinyl sulfone.[13] A couple of years ago, bacterial cellulose (BC) started to be used for hydrogel-based super-adsorbents,[14] which were dedicated at first to protein separations. Bacterial cellulose differs from vegetal cellulose through the fact that it is produced by bacteria, such as: *Acetobacter*, *Sarcina ventriculi* and *Agrobacterium*, and has improved mechanical strength, higher water absorption capacity and higher crystallinity.[15] Some studies explained this particular difference by the fact that aerobic bacteria produce nano-fibrils of cellulose with a denser structure, which implicitly leads to considerable improvement of properties.[16,17] At present, BC-based hydrogels are highly studied and produced for biomedical applications and drug delivery, but no reports

[a]National Research and Development Institute for Chemistry and Petrochemistry-ICECHIM, Polymers Department, Advanced Polymer Materials and Polymer Recycling Group, Bucharest, Romania. E-mail: andr.sarbu@gmail.com; iordachev.icechim@gmail.com; Tel: +40-724237351; +40-755159896

[b]Institute of Physical Chemistry of the Romanian Academy "Ilie Murgulescu", Bucharest, Romania

[c]University "Politehnica" of Bucharest, Faculty of Applied Chemistry and Materials Science, Bioresources and Polymer Science Department, Bucharest, Romania

were retrieved for BC-based hydrogels for agriculture use.[18–22] As a result, interpenetrated polymer networks (IPNs) of BC and poly(acrylic acid-*co*-N,N′-methylene-bis-acrylamide) were prepared and described in this paper for the first time, in order to deliver robust materials with various shapes, dimensions and adsorption–desorption profiles of fertilizers, adequate for agriculture applications. Interpenetrated polymer network (IPN) hydrogels are defined as a combination of two or more polymer networks which are formed by synthesis in juxtaposition.[23,24] Many investigations were performed to synthesis new structures of IPN hydrogels based on synthetic polymers and polysaccharides.[25] The most employed polysaccharides consist in: chitosan,[26,27] alginate,[28–30] starch,[31–34] salecan,[35] cellulose,[36,37] carboxymethylcellulose,[38,39] *etc.* It can be noted that IPNs with BC and synthetic polymers like acrylic resin,[19] poly(lactic acid),[20] meth/acrylic acid,[21,22] acrylic acid,[11] and acrylamide,[40] were only synthesized so far by ultra-violet mediated our irradiation procedures and used for non-related agriculture applications. In most of the reports, the bacterial cellulose was lyophilised before use, leading practically to paper-like sheets, which are hard to process for yielding IPNs. Kramer and co-workers[21] obtained new IPN composite hydrogels based on non-lyophilized BC and acrylic monomers (acrylic acid, 2-ethyl-hexyl acrylate, 2-hydroxyethyl methacrylate, N-vinyl pyrrolidone) by photo-polymerisation inside an ethanol-swollen nano-fibber network. Yet, the use of ethanol instead of water reduced the swelling ability of final IPNs. Plus, ethanol is more expensive than water and not as friendly. Hence, the present study describes the synthesis of composite hydrogels and xerogels based on bacterial cellulose and poly(acrylic acid-*co*-N,N′-methylene-bis-acrylamide) *via* "*in situ*" radical copolymerisation as a new and direct synthesis method for IPNs. The final properties of the BC-IPN composite hydrogels were optimized in terms of water adsorption capacity, mechanical strength, and controlled release profile of the liquid fertilizer (LFs) in water. It is also worth mentioning, that fertilizers are usually delivered by the manufacturer as aqueous solutions because are generally easier to transport than the solid fertilizers (SF) and cause fewer work problems in handling and application.[41,42] In this respect, the new BC-IPN composite xerogels (dried hydrogels) with high water and SF retention capacity can also represent a safer method for transportation and a less complicated route for soil application.

2 Experimental section

2.1. Materials

The monomer, acrylic acid (AA, Sigma-Aldrich, 99%) was distilled at vacuum before use, and the crosslinker, N,N′-methylene-bis-acrylamide (MBA, Sigma-Aldrich, 99%) was used as received. Ammonia aqueous solutions 25% was purchased from Chimopar SA and the radical polymerisation redox system, composed of potassium persulphate (KPS, 99%) and sodium metabisulphide (MS, 97%) was procured from Acros Organics. Bacterial cellulose (BC) was obtained by collaborators from the University "Politehnica" of Bucharest in static culture using fructose as carbon source and pollen as nitrogen source[43] and

delivered in acetic acid. The foliar chemical fertilizer (with microelements) encapsulated into the new BC-IPN composite hydrogels was KRISTALON and provided in solid state (SF).

2.2. Preparation of IPN composite hydrogels based on bacterial cellulose and poly(acrylic acid-*co*-N,N′-methylene-bis-acrylamide)

The synthesis of the IPN hydrogels was accomplished through radical copolymerization of acrylic acid with N,N′-methylene-bis-acrylamide (MBA) in the presence of non-lyophilized bacterial cellulose, in aqueous media, initiated by potassium persulphate (KPS) and sodium metabisulphite (MS) redox system (as described in Scheme 1). The bacterial cellulose (BC), obtained in static culture,[43] was shredded for 10 minutes with a blender until 1–2 mm particles of BC were obtained. Subsequently, the BC aqueous solution was filtered on filter paper for 2 hours (to reduce the water content to 40–30% relative to the total amount of water). Using the resulted swollen BC, a stock bacterial cellulose solution containing AA (30% neutralized with NH_3) and MBA was prepared in 10 mL glass vials with a diameter of 10 mm. Two sets of hydrogels were prepared: one containing the LF (4 mL solution, 30 g SF/L water) and another only distilled water (4 mL) as control sample. The vials with the resulting mixtures were placed in an ultrasonic bath at room temperature for allowing the monomers to be absorbed into the BC nanostructured network. After 3 hours, the redox initiation system (KPS/MS) was added and the vials were placed back into the ultrasonic bath for homogenisation (approximately 1 min). Afterward, the vials were purged with nitrogen gas (for about 3 min) to remove oxygen, sealed by rubber septa and then placed into an oil bath at 30 °C for 24 hours. At the end, the tubes were removed from the heating bath, broken and the hydrogel rods were cut into small disk-shape pieces of about 1 cm thick. Slices of each hydrogel type were placed into an excess of distilled water for 5 days at room temperature. The water was changed daily in order to remove the unreacted monomer. After this
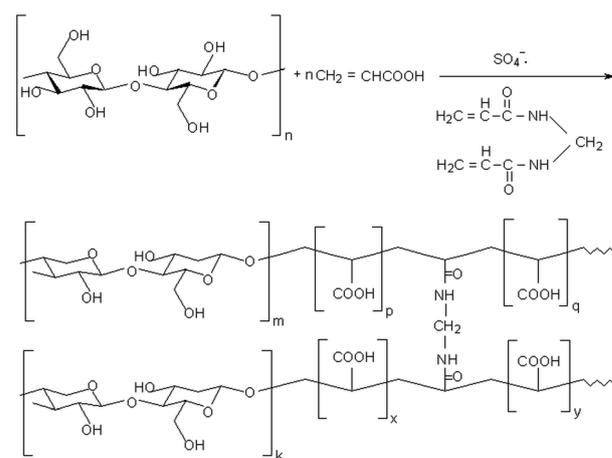
Scheme 1 Synthesis mechanism of the interpenetrated polymer networks (IPNs) of BC and poly(acrylic acid-*co*-N,N′-methylene-bis-acrylamide) by free-radical inducing polymerization.

purification – swelling period, the swollen hydrogels were placed into an oven at 50 °C until constant weight, to determine the swelling degree. BC was lyophilized and grounded, using ball milling, to obtain fine particles adequate for Fourier transform infrared spectroscopy (FTIR), thermo-gravimetric (TGA), derivative thermo-gravimetric (DTG) analysis and scanning electron microscopy (SEM). Same investigations were considered for the BC-IPN composite hydrogels and the control hydrogels, for determining the influence of reactants concentration upon the overall adsorption properties. Plus, the mechanical properties and rheological behaviour of the swollen composite hydrogels were also evaluated, to highlight the improvement of the properties of interest (e.g. mechanical stability) for further agriculture use.

2.3. Determination of the swelling degree

The swelling degree (SD) of the control and BC-IPN composite hydrogels was determined by placing the hydrogel disks in distilled water at room temperature. This procedure was preferred because during swelling of hydrogels the unreacted monomers are also released. After 5 days, the hydrogels were recovered by vacuum filtration using a G1 filtering crucible, weighed (W_h) and dried to constant weight (W_x) at 50 °C in an oven at atmospheric pressure. According to eqn (1), the swelling degree (SD) was calculated as the ratio between the amount of water absorbed by the hydrogel during the purification – swelling period and the amount of dried polymer (xerogel).

$$SD(\text{g water/g dry polymer}) = \frac{W_h - W_x}{W_x} \times 100 \qquad (1)$$

2.4. Characterization methods

The FTIR spectra of the samples were recorded on Nicolet FTIR Model 500 by acquiring 32 scans with 4 cm^{-1} resolution in 4000–400 cm^{-1} region, on a KBr pellet.

The thermo-gravimetric analyses (TGA) were performed on Thermal Analysis SDT600 instrument, by heating about 5 to 10 mg of sample hydrogel from room temperature to 700 °C at a constant heating rate of 10 °C min^{-1}, under nitrogen flow.

The X-ray diffraction (XRD) patterns were collected with a SmartLab diffractometer (Rigaku, Japan) equipped with Cu Kα radiation (wavelength $k = 0.1541$ nm). The scanned range was 2 h = 2–90°, with a scan speed of 1° min^{-1}.

The scanning electron microscopy (SEM) analyses were carried out on FEI Quanta 3D FEG from Phillips, at an acceleration voltage of 20 kV (SE-secondary electrons).

Rheological measurements were performed on Bohlin Gemini 150 - Malvern Instruments at 25 °C, at a constant shear stress of 100 Pa and a frequency of 1 Hz, using parallel plate geometry 20 mm with a gap of 500 μm. The strain values were chosen in the linear visco-elastic range, where the storage modulus (G') and the loss modulus (G'') do not depend on the strain amplitude. The measurements were carried out on hydrogel particles previously swollen in distilled water for 24 h.

The surface water was removed from hydrogels with filter paper.[44]

For determining the LF release profiles, supernatants were analysed using DIONEX ICS 3000 Instrument for ion chromatography (produced in SUA), equipped with anion separation column, IonPac AS22 4 × 250 mm; pre-column IonPac AG22 4 × 50 mm; suppressor of anions ASRS 300 × 4 mm; conductivity detector; isocratic pump – 1 mL min^{-1} flow rate, injection volume of 1 mL; injection loop of 0.25 μL. For purification, the samples were filtered on 0.45 μm filters.

2.5. Controlled release profiles of LF

For determining the release profiles of the LF, 0.5 g of BC-PAA IPN composite xerogel with encapsulated LF was grounded and contacted with 100 mL of distilled water at room temperature. 1 mL of supernatant was taken at various times (for 3 days) and diluted with 9 mL of stock solution before being injected into the ion chromatograph.

3 Results and discussions

3.1. Synthesis of composite hydrogels

The research was aimed at obtaining BC-IPN composite hydrogels and xerogels having various amounts of incorporated solid fertilizer (SF). The composite hydrogels (recipes given in Table 1) were noted either X-LF-BC-PAA, where X represents the amount of liquid fertilizer (LF), obtained from X g of SF in 0.5 L of water, or LF-BC-PAA (YMBA), where Y represents the wt% of MBA crosslinker relative to AA.

3.2. FT-IR spectroscopy

FTIR spectra of control xerogels (LF-PAA) and of composite xerogels (LF-BC-PAA) are compared in Fig. 1 to that of BC, of polyacrylic acid (PAA) alone and of LF. BC spectrum shows characteristic bands at 3332 cm^{-1} and 2894 cm^{-1} wavelength corresponding to the stretching vibration of OH bonds and to the CH bonds in methylene groups, respectively. Bacterial cellulose presents characteristic bands at the following wavelengths: 1323 cm^{-1} (CH$_2$ group), 1104 cm^{-1} asymmetric vibration of the glycoside ring and 1057 cm^{-1} vibration of the C–O group for primary and secondary alcohols.

The bands registered at 2926 cm^{-1} and 2886 cm^{-1} for the control PAA xerogel were associated with the characteristic stretching vibration CH in methylene and methylidene groups. The band at 1715 cm^{-1} was attributed to the protonated carboxyl groups that form cyclic dimmers, while the two bands, near 1634 cm^{-1} and 1455 cm^{-1} were characteristic for the asymmetric and symmetric stretching vibrations of C=O bonds, in the protonated carboxyl groups. The broad band ranging from 3100 to 3700 cm^{-1} was due to the presence of intramolecular hydrogen bonds formed by the carboxylic moieties of AA.[45] For the encapsulated fertilizer, characteristic bands were spotted at 3300 cm^{-1} and 3500 cm^{-1}, which corresponded to the O–H and N–H stretching in the dehydrogenated ammonium phosphate and in the dehydrogenated potassium phosphate, respectively, found in the fertilizer

Table 1 Recipes of BC–IPN composite hydrogels with various LF concentrations and MBA contents[a]

Sample	[BC] (% rel. to [AA])	LF (mL) (sol. X g SF/0.5 L H_2O)	[MBA] (% M rel. to [AA])
2.5-LF-BC-PAA	100	2.5	0.5
5-LF-BC-PAA		5	
10-LF-BC-PAA		10	
15-LF-BC-PAA		15	

[a] [AA-NH$_4^+$] = 6 M/L and [KPS/MS] = 1% rel. to [AA], for all recipes. [b] Samples without BC were also prepared as control and noted as LF-PAA (YMBA). [c] Samples without BC and SF were also prepared as control and noted as PAA (YMBA).

Sample	[BC][b] (% rel. to [AA])	LF[c] (mL) (sol. 10 g SF/L H_2O)	[MBA] (% rel. to [AA])
LF-BC-PAA (0.1MBA)	100	0.5	0.1
LF-BC-PAA(0.15MBA)			0.15
LF-BC-PAA (0.2MBA)			0.2
LF-BC-PAA (0.3MBA)			0.3
LF-BC-PAA (0.4MBA)			0.4
LF-BC-PAA (0.5MBA)			0.5

formulation. The absorption band at 1383 cm^{-1} was attributed to the presence of P=O double bond and that of P–OH gagging was registered at 1140 cm^{-1}. More characteristic bands from the dehydrogenated ammonium phosphate, like stretching of HO–P–OH, O–N=P and –O–NO$_2$ bonds were also recorded at 1074 cm^{-1} and between the 700–900 cm^{-1} wavelength range.[15] Thus, the spectrum of control LF-PAA and of composite LF-BC-PAA xerogel presented the characteristic bands of both the PAA and the FS components. Additionally, the spectrum of the composite LF-BC-PAA xerogel also indicated the presence of BC at 1057 cm^{-1}, band corresponding to the stretching vibration of C–O bond (for primary and secondary alcohols).

3.3. Thermo-gravimetric profiles (TGA/DTG)

Thermograms and DTG profiles of synthesized xerogels are given in Fig. 2. The TGA plots of control PAA hydrogels are complex (Fig. 2a), decomposing in three main steps with a maximum mass loss of 82.11%. The first decomposition step, with 8.07% mass loss, recorded a maximum at 120 °C and

Fig. 1 FTIR spectra of BC, PAA, LF, LF-PAA and LF-BC-PAA.

corresponded to a dehydration process (DTG curve, Fig. 2b). Further degradation occurred at 231 °C, with 23.54% mass loss (associated with dihydroxylation of PAA), and at 395 °C, with 50.50% mass loss, which included the loss of short chain fragments (exothermic chain scission of the polymer).[45,46] BC alone degraded in a single step at 324 °C (endothermic degradation process).[47] Further on, Fig. 2b suggested that BC-PAA without LF was homogenous and degraded in three steps similar to those of the PAA. The decomposition peak from 250 °C resemble with the dihydroxylation step of PAA and with the on-set of BC decomposition step, suggesting that the on-set of PAA dihydroxylation in the composite hydrogels began at a higher temperature due to PAA-BC IPN formation with more compact structure with higher thermal stability.[11]

Fig. 3 shows the TGA and DTG curves of control xerogels (LF-PAA) and of composite xerogels (LF-BC-PAA) with fertilizer. LF-PAA decomposed in three major stages (Fig. 2b), as follows: at 77 °C, with a mass loss of 5.93% associated with the dehydration process; at 227 °C, with a mass loss of 22.10% (dihydroxylation/decarboxylation of PAA) followed by the third stage at 394 °C with a mass loss of 54.92% (degradation of the polymer backbone). From the TGA curves (Fig. 3a), a total mass loss of 88.92% was attained for this blank xerogel sample. The composite LF-BC-PAA xerogel presented similar TGA and DTG profiles with that of LF-PAA, but with no distinctive peaks of BC, which also suggested the formation of IPNs. Plus, the weight loss in this case was lower, i.e. 82.95%. Therefore, it can be stated that the presence of BC led to the formation of additional crosslinking points with the polymeric AA network creating IPNs with higher crosslinking degrees, and thus, with improved thermal stability of the hybrid backbone (decomposition occurring at 399 °C, Fig. 3b). As described further, the formation of IPNs also led to lower swelling degrees but improved mechanical strength of hydrogels.
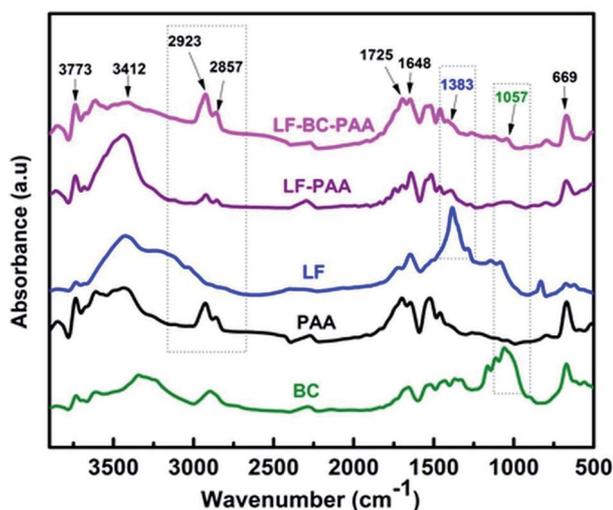
3.4. XRD – X-ray diffraction

The XRD diffraction patterns of control composite xerogels (BC-PAA and LF-BC-PAA) are compared in Fig. 4 to that of simple BC
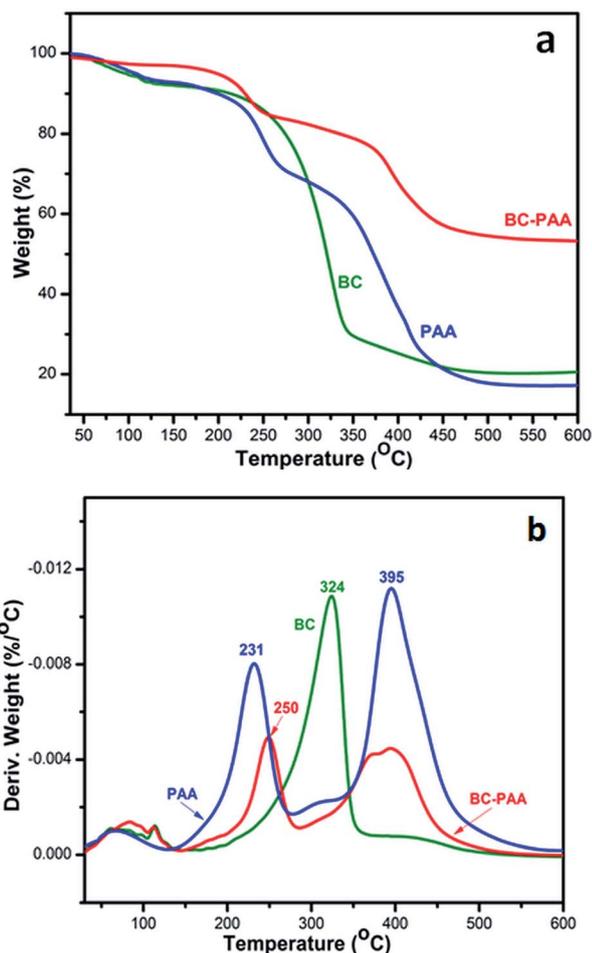
Fig. 2   TGA (a) and DTG (b) curves of BC, PAA and BC-PAA.
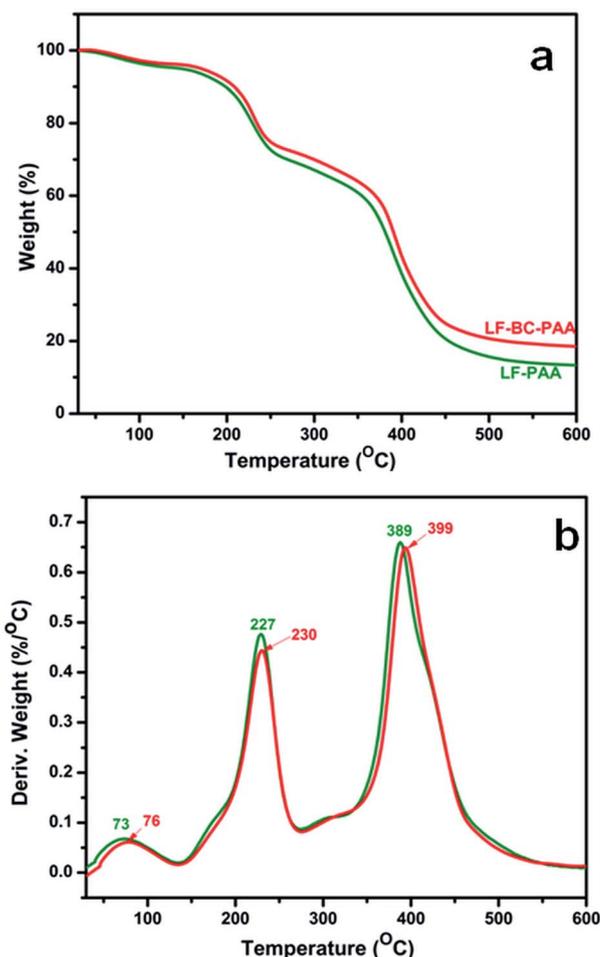

Fig. 3   TGA (a) and DTG (b) profiles of control xerogels LF-PAA and of composite xerogels LF-BC-PAA.

and PAA alone. The bacterial cellulose is a semi-crystalline material that usually produces three major characteristic crystalline peaks: at 2θ – 14.2 and 22.7 along with a weak middle peak at 16,6 corresponding to the (1−10), (200) and (110) crystalline planes of the cellulose 1β structure.[48] The structure of PAA is amorphous and presents a broad peak at 2θ – 17.8. Further on, analysing the XRD pattern of the composite xerogels (BC-PAA and LF-BC-PAA), broad peaks related to PAA were spotted at 2θ – 17.6 and 17.9, respectively. However, the characteristic peaks of crystalline BC disappeared and a hump, characteristic for amorphous zones, appeared instead. The reason for this observation is simple. The network interpenetration of PAA with BC resulted in the destruction of the specific crystalline regions of BC alone;[49] and thus, confirming the proposed polymerization mechanism that led to the formation of IPNs.[50]

3.5.   Morphology of xerogels

In Fig. 5 the SEM micrographs of the freeze-dried composite hydrogels with embedded fertilizer are presented. The images clearly highlight the presence of both the BC and that of the fertilizer in the structure of composite hydrogel. Fig. 5a reveals

the homogeneous and macroporous morphologies of the freeze-dried PAA hydrogel, with pore size in the range of several hundred microns, which seemed to be causing the high water absorption. Regarding the control hydrogel with encapsulated fertilizer LF-PAA (Fig. 5b), the surface presented a porous morphology with open and interconnected channels in the range of tens of microns. Herein, the SF is homogeneously deposited on the walls of the PAA hydrogel network. The porous structure is defined by the average distance between crosslinking points along the polymer chains comprising the hydrogel network.[51] Hence, the formation of pores was influenced by the addition of cross-linker as shown in Scheme 1. In this case, graft copolymerization of bacterial cellulose (BC) with acrylic acid (AA) was performed by free-radical inducing polymerization, initiated by the redox initiation system potassium persulphate/sodium metabisulphide (KPS/MS). $SO_4^{\cdot-}$ generated free radical sites, which reacted with the AA monomer to form graft copolymers. Thereby, the final composite hydrogel structures were obtained by introducing N'-methylene-bisacrylamide (MBA) as cross-linker. This latter ingredient led to the formation of swollen 3D network structures.[52] By the addition of BC (Fig. 5c), the homogeneity and the pore size of the
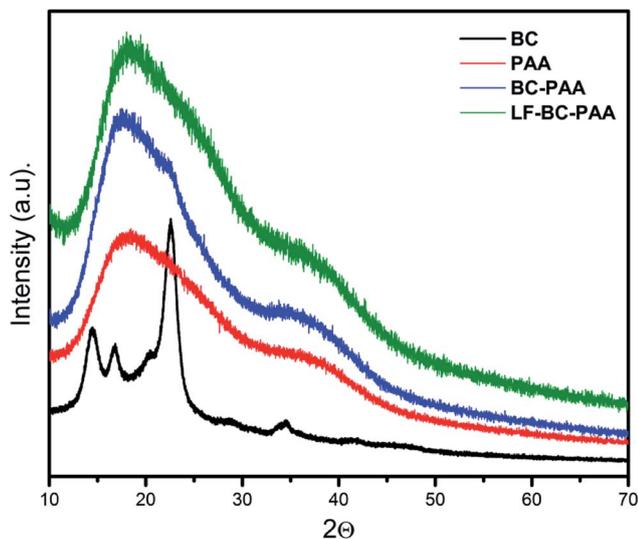
Fig. 4   XRD diffraction patents of the BC, PAA, BC-PAA and LF-BC-PAA.

composite hydrogel decreased, which was due to the swelling of BC fibbers during impregnation with AA and to the subsequent polymerization/crosslinking in the fibber structure (Fig. 5c). The SEM images also revealed the characteristic fibrous and multilayered arrangement of the lyophilized and milled BC,[53] (in Fig. 5c) and the solid fertilizer crystalline structure (in Fig. S1, Appendix A†); these stacked crystals are composed of ammonium and potassium phosphates and microelements (B, Fe, Zn, Cu, Mn and Mo), according to the fertilizer formulation. Yet, the morphological observations suggest that the porous structure of the composite hydrogels facilitated the diffusion of

water in all directions, making these hydrogels suitable for controlled release applications.[11] It was also observed that the structures of PAA and of BC were interpenetrated; and thus, confirming again the polymerization mechanism that led to the formation of IPNs. Moreover, the fertilizer was spotted on the surface of the composite xerogel and also within the interpenetrated polymer networks and pores.

3.5. The influence of MBA concentration upon the swelling degree of hydrogels

The synthesized hydrogels were submitted to swelling determinations, in order to quantify the influence of the crosslinker concentration (MBA) upon the swelling degree of hydrogels, SD (or water absorption capacity). As previously mentioned, 6 molar concentrations of MBA (Table 1) were used to obtain hydrogels with different [MBA]/[PAA] ratios. In order to check the influence of MBA concentration upon the SD of hydrogels, [MBA] concentration was varied while all other components, i.e. [AA] and [KPS/MS]/[AA], remained constant.

Fig. 6 suggests that high crosslinker amounts led to high crosslinking degrees, and implicitly, to low swelling degrees. It can also be mentioned that control hydrogels with PAA alone presented the highest degrees of swelling (Fig. 6, red columns). With the change of the polymerization medium, from distilled water to liquid fertilizer solution (represented here by the LF-PAA system), a significant decrease of the swelling degree was observed (Fig. 6 yellow columns). This can be due to the presence of Fe, Zn, Cu, Mn, and Mo microelements in the LF. It is known that the presence of ions (Fe^{2+}, Zn^{2+}, Cu^{2+} etc.) in the hydrogel structure leads to a decrease of the swelling degree. James and Richards[54] have suggested that these bivalent cations develop strong interactions with the polymeric network and are able to remove water molecules trapped within the polymer network.

Further introduction of BC in the hydrogel structure has yield even lower swelling degrees (Fig. 6, blue columns). This is
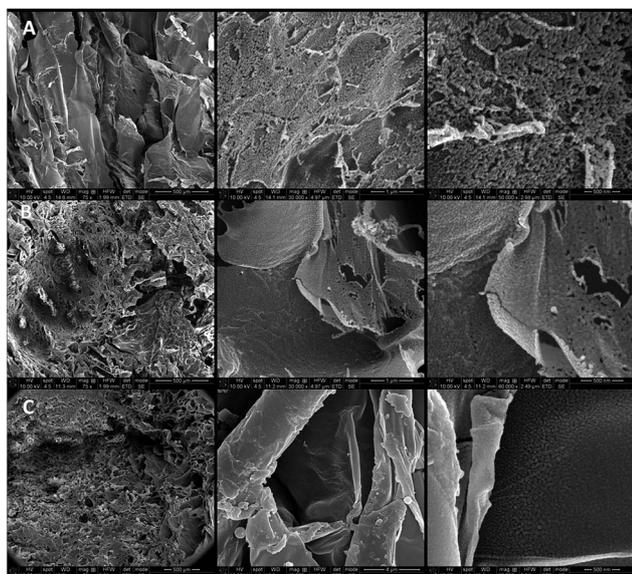

Fig. 5   Morphology of freeze-dried control and composite hydrogel, at various scales, in the following order: (a) PAA control xerogel; (b) control xerogels with fertilizer, LF-PAA; and (c) composite xerogels with fertilizer, LF-BC-PAA.
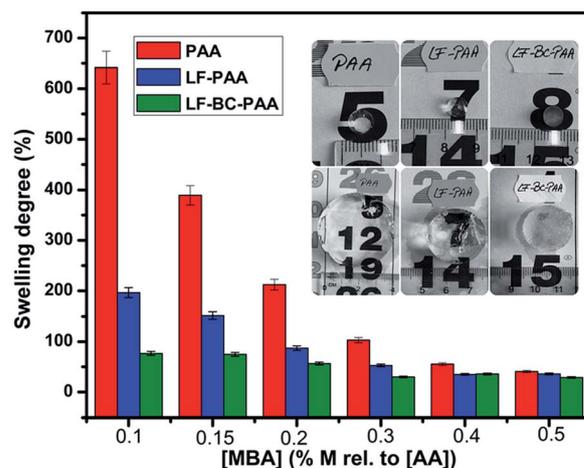

Fig. 6   The influence of MBA concentration upon the swelling degree, SD of hydrogels (mean values of 2 measurements); hydrogels before and after swelling (medallion).

not surprising at all because additional crosslinking points are generated during IPNs formation, as suggested by TGA and SEM measurements, as well. Herein, the SD decrease was wanted as it may result in a slower rate of fertilizer diffusion in water, and hence, in a more controlled release. In Fig. 6, medallion, it can also be observed that the LF-BC-PAA hydrogel presented a lower transparency degree, attesting morphological and structural changes caused by BC interpenetration.

3.6. The influence of the SF concentration upon the swelling degree of hydrogels

The influence of the SF amount upon the degree of swelling was also evaluated. In this respect, 4 concentrations of fertilizer were used (Table 1) in order to obtain composite hydrogels with different LF concentrations. Thus, we considered the fertilizer concentrations recommended by the manufacturer and several LF solutions, with various [LF]/[H$_2$O] ratios (2.5/500, 5/500, 10/500 and 15/500 in g mL^{-1}) were formulated. Similar to the MBA variance study, the concentration of SF was altered while all other components, *i.e.* [AA], [MBA]/[AA] and [KPS/MS]/[AA] were maintained constant.

Fig. 7 indicates a decrease of the SD for the control and the composite hydrogels, LF-PAA and LF-BC-PAA respectively, with the increase of the SF. These results were consistent with the previous explanation regarding the effect of ions (Fe^{2+}, Zn^{2+}, Cu^{2+} *etc.*) that are found in the SF formulation and contribute to water elimination.[31] Yet, a more pronounced decrease of the SD, of about 40% was registered for the control samples LF-PAA (Fig. 7, Red Columns). With the insertion of BC into the hydrogel structure this effect is slightly attenuated, the SD decreasing only by 12% (Fig. 7, green columns).

3.7. Rheological behaviour of hydrogels

Rheological measurements were performed at 25 °C, using parallel plate geometry. The shear stress value, *i.e.* 0.01 Pa was chosen in the linear visco-elasticity (LVE) region, where the

elasticity modulus (G') and the viscosity modulus (G'') are independent of the shear stress amplitude.

The frequency sweep measurements allowed the visco-elastic characterization of the hydrogels at 25 °C (Fig. 8a and b). In all the cases, the elasticity modulus was greater than the viscosity module ($G' > G''$) resulting in a predominant elastic character of the hydrogel samples. These results are promising for obtaining hydrogel materials with increased mechanical stiffness. It can also be noted that the value of the elasticity modulus increased gradually with the frequency, indicating a slow relaxation (characteristic for rigid materials). So, this result was also useful because it suggested that an enhancement of the mechanical strength of composites hydrogels has occurred. In Fig. 8a, an obvious increase of the elasticity modulus (G') was observed for BC and for the composite hydrogels (LF-BC-PAA) as compared to the control hydrogels (LF-PAA). For LF-BC-PAA composite hydrogels, synthesized with different concentrations of cross-linker (MBA) (Fig. 8b), the elasticity modulus G' increased with the concentration of MBA. The results are in line with the literature data.[55] These results were also consistent with the SD values determined for the LF-BC-PAA, which suggested that formation of IPNs induced important modifications of the
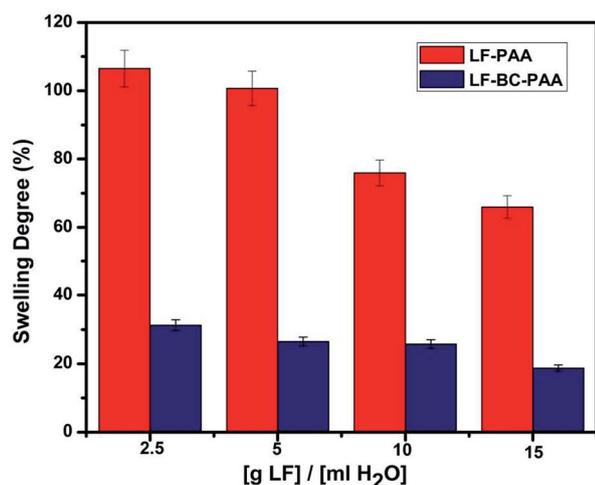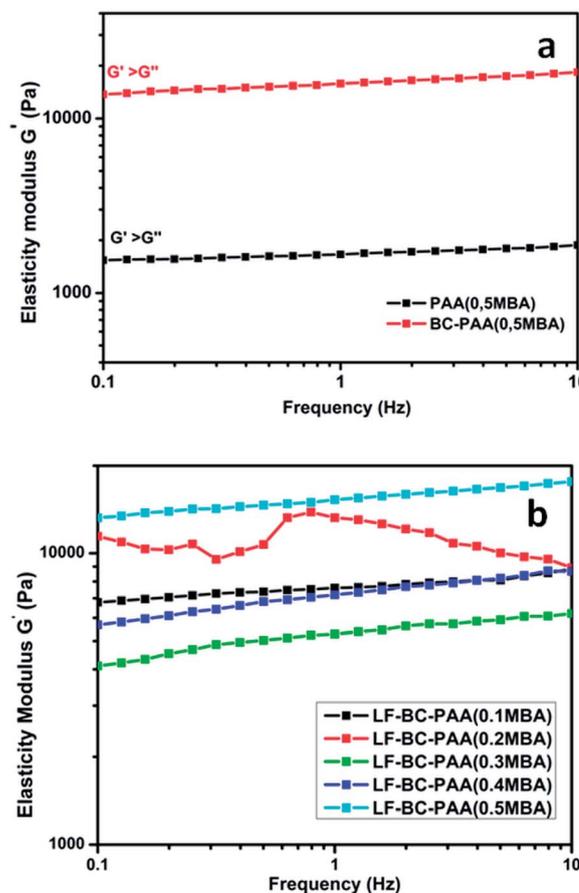

Fig. 8 Rheological determinations: (a) elasticity modulus (G') relative to the frequency, characteristic for control LF-PAA and composite LF-BC-PAA hydrogels; (b) elasticity modulus (G') relative to the frequency, characteristic for composite LF-BC-PAA hydrogels with various crosslinker ratios (YMBA).

Fig. 7 The influence of the SF concentration upon the SD of hydrogels (mean values of 2 measurements).

hydrogel properties. Hence, these hybrid structures also seem to contribute significantly to the increase of the elasticity modulus, G', for the composite hydrogels. In conclusion, we can state that BC addition to the hydrogels improved significantly the mechanical stiffness and stability of the composite hydrogels.

3.8. Controlled release profiles of the LF

The release profiles of the encapsulated fertilizer were determined using Ion Chromatography (IC). In this respect, a standard solution with seven anions, *i.e.* F^-: 20 mg L^{-1}; SO_4^{2-}, Cl^-, NO^{2-}, NO^{3-}, Br^-: 100 mg L^{-1}; PO_4^{3-}: 200 mg L^{-1} (DIONEX from THERMO SCIENTIFIC) was used. Calibration was performed for the concentration ranges: 0.1–6.0 mg L^{-1} (NO^{3-}) and 0.2–12 mg L^{-1} (PO_4^{3-}). From the calibration measurements (Fig. S2, Appendix A†), the following coefficients of determination (%) were obtained: 99.9990 (NO^{3-}) and 99.9996 (PO_4^{3-}). The initial concentration of the ions in the fertilizer solution (15 g/500 mL) was: NO^{3-}: 17.25 g L^{-1} and PO_4^{3-}: 1.72 g L^{-1}. The results obtained by IC for the control LF-PAA and composite LF-BC-PAA hydrogels are given in Table S1, Appendix A.†
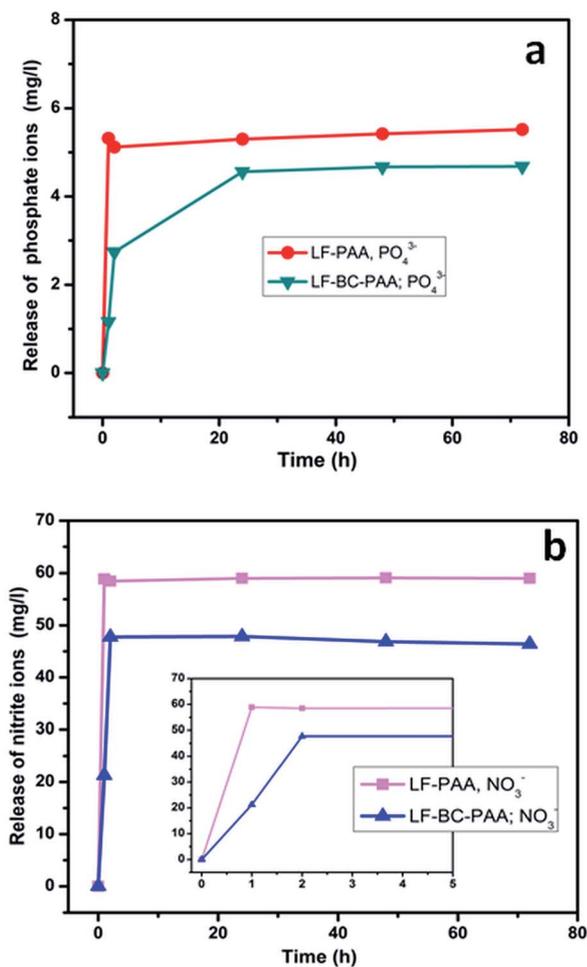

Fig. 9 LF release profiles in water, in terms phosphate ions – (a) and of nitrate ions – (b), during 3 days, for the control LF-PAA and the composite LF-BC-PAA hydrogels.

Results show that a sharp release of nitrite and phosphate ions (Fig. 9) was registered for the control samples in the first hour of contact with water. The LF release profile for the composite hydrogels was similar; yet, it indicated a slower release rate of fertilizers, having a 2 h stabilization period compared to the 1 h period registered for the control sample. While for the composite hydrogels LF-BC-PAA, the rate and amounts of released nitrate and phosphate were lower and relative constant in 72 hours, the results obtained for the control PAA hydrogels (Fig. 9) indicated a faster release rate of fertilizers (as the released amounts of fertilizer were higher each day). The results were somehow expected, because the addition of BC in the composites led to denser polymeric networks; and thus, to a hampered release of the fertilizer from the LF-BC-PAA hydrogels. As literature suggested, the nutrient release mechanism from LF-BC-PAA hydrogels can be described in three main stages: (i) water adsorption in the BC-PAA bulk structure, (ii) nutrient slow dissolution by water, and (iii) nutrient delivery in the exterior medium by diffusion from the BC-PAA hydrogels.[33]

4. Conclusions

This paper, describes the successful synthesis of the new composite hydrogels by radical copolymerization, based on bacterial cellulose and poly(acrylic acid-*co-N*,*N*′-methylene-bis-acrylamide) with interpenetrated polymer networks (IPNs). The liquid fertilizer (LF) was encapsulated directly into the composite hydrogels during synthesis and the micrographs showed a good distribution of the solid fertilizer particles inside the IPN of the composite xerogels. Along electron microscopy, thermal analyses of composite xerogels also highlighted the formation of IPNs which improved the thermal stability relative to the precursors. The swelling degrees of the composite LF-BC-PAA hydrogels were highly dependent upon the MBA ratio due to the fact crosslinking reduces the access of water into the polymer network. Yet, the concentration of liquid fertilizer LF also had similar effects because of Fe, Zn, Cu and Mn ions, which seem to establish strong interactions with the polymer network as in a physical crosslinking. Further on, comparing the elasticity and the viscosity modules, G' and G'' respectively, it was concluded that the LF-BC-PAA composites are more rigid and stiff than the control hydrogels due to BC addition and of course IPN formation. Also, thanks to IPN formation the release profile of encapsulated fertilizer tracked by ion chromatography was quite different; composite LF-BC-PAA presenting a slower rate of LF diffusion by a more controlled mechanism. Therefore, the overall properties of composite LF-BC-PAA hydrogels were definitely optimized and can be used in agriculture practices.

Conflicts of interest

There are no conflicts to declare.

Acknowledgements

consortium (ProWsper Project no. 39/2017) financed under the ERA-NET Cofund WaterWorks2015 Call. This ERA-NET is an integral part of the 2016 Joint Activities developed by the Water Challenges for a Changing World Joint Programme Initiative (Water JPI).

Notes and references

1 M. Teodorescu, A. Lungu, P. O. Stanescu and C. Neamțu, *Ind. Eng. Chem. Res.*, 2009, **48**, 6527–6534.

2 O. Wichterle and D. Lim, *Nature*, 1960, **185**, 117–118.

3 G. D. Nicodemus and S. J. Bryant, *Tissue Eng., Part B*, 2008, **14**, 149–165.

4 S. Sampath, N. A. Choudhury and A. K. Shukla, *J. Chem. Sci.*, 2009, **121**, 727–734.

5 E. Brinkman, L. Van der Does and A. Bantjes, *Biomaterials*, 1991, **12**, 63–70.

6 K. S. Kazanskii and S. A. Dubrovskii, *Adv. Polym. Sci.*, 1992, **104**, 97–133.

7 A. Shaviv, *Adv. Agron.*, 2001, **71**, 1–49.

8 W. E. Rudzinski, A. M. Dave, U. H. Vaishnav, S. G. Kumbar, A. R. Kulkarni and T. M. Aminabhavi, *Des. Monomers Polym.*, 2002, **5**, 39–65.

9 M. Liu, R. Liang, F. Zhan, Z. Liu and A. Niu, *Polym. Adv. Technol.*, 2006, **17**, 430–438.

10 D. Saraydin, E. Karadag and O. Güven, *Polym. Bull.*, 2000, **45**, 287–294.

11 M. C. I. M. Amin, N. Ahmad, N. Halib and I. Ahmad, *Carbohydr. Polym.*, 2012, **88**, 465–473.

12 W. Zoua, L. Yua, X. Liu, L. Chen, X. Zhang, D. Qiao and R. Zhang, *Carbohydr. Polym.*, 2012, **87**, 1583–1588.

13 A. Sannino, G. Mensitieri and L. Nicolais, *J. Appl. Polym. Sci.*, 2004, **91**, 3791–3796.

14 T. Oshima, S. Taguchi, K. Ohe and Y. Baba, *Carbohydr. Polym.*, 2011, **83**, 953–958.

15 E. J. Vandamme, S. De Baetsa, A. Vanbaelenb, K. Jorisa and P. De Wulfa, *Polym. Degrad. Stab.*, 1998, **59**, 93–99.

16 R. J. B. Pinto, M. C. Neves, C. P. Neto and T. Trindade, *Composites – New Trends and Developments*, ed. F. Ebrahimi, 2nd edn, 2012, ISBN 978-953-51-0762-0.

17 S. Khan, M. U. Islam, M. W. Ullah, M. Ikram, F. Subhan, Y. Kim, J. H. Jang, S. Yoonc and J. K. Park, *RSC Adv.*, 2015, **5**, 84565–84573.

18 P. Matricardi, C. Di Meo, T. Coviello, W. E. Hennink and F. Alhaique, *Adv. Drug Delivery Rev.*, 2013, **65**, 1172–1187.

19 E. Trovatti, L. Oliveira, C. S. R. Freire, A. J. D. Silvestre, C. P. Neto, J. J. C. C. Pinto and A. Gandini, *Compos. Sci. Technol.*, 2010, **70**, 1148–1153.

20 M. Martínez-Sanz, M. A. Abdelwahab, A. Lopez-Rubio, J. M. Lagaron, E. Chiellini, T. G. Williams, D. F. Wood, W. J. Orts and S. H. Imam, *Eur. Polym. J.*, 2013, **49**, 2062–2072.

21 F. Kramer, D. K. D. Schumann, N. Hessler, F. Wesarg, W. Fried and D. Stadermann, *Macromolecular Symposium.*, 2006, **244**, 136–148.

22 R. Hobzova, M. Duskova-Smrckova, J. Michalek, E. Karpushkin and P. Gatenholm, *Polym. Int.*, 2012, **61**, 1193–1201.

23 L. H. Sperling, D. Klempner and L. A. Utracki, *Interpenetrating Polymer Networks*, American Chemical Society, Washington, DC, 1994.

24 R. Bera, A. Dey, A. Datta Sarma and D. Chakrabarty, *RSC Adv.*, 2015, **5**, 75870–75880.

25 E. S. Dragan, *Chem. Eng. J.*, 2014, **243**, 572–590.

26 L. Yin, L. Fei, F. Cui, C. Tang and C. Yin, *Biomaterials*, 2007, **28**, 1258–1266.

27 S. Chen, M. Liu, S. Jin and Y. Chen, *J. Appl. Polym. Sci.*, 2005, **98**, 1720–1726.

28 L. Yin, L. Fei, F. Cui, C. Tang and C. Yin, *Polym. Int.*, 2007, **56**, 1563–1571.

29 H. Lin, J. Zhou, C. Yingde and S. Gunasekaran, *J. Appl. Polym. Sci.*, 2010, **115**, 3161–3167.

30 R. Mahou and C. Wandrey, *Macromolecules*, 2010, **43**, 1371–1378.

31 B. Zhu, D. Ma, J. Wang and S. Zhang, *Carbohydr. Polym.*, 2015, **133**, 448–455.

32 D. Qiao, H. Liu, L. Yua, X. Baoa, G. P. Simon, E. Petinakis and L. Chen, *Carbohydr. Polym.*, 2016, **147**, 146–154.

33 S. Jin, Y. Wang, J. He, Y. Yang, X. Yu and G. Yue, *J. Appl. Polym. Sci.*, 2013, **128**, 407–415.

34 E. S. Dragan and D. F. Apopei, *Chem. Eng. J.*, 2011, **178**, 252–263.

35 X. Hu, W. Wei, X. Qi, H. Yu, L. Feng, J. Li, S. Wang, J. Zhang and W. Dong, *J. Mater. Chem. B*, 2015, **3**, 2685–2697.

36 J. Wang, X. Zhou and H. Xiao, *Carbohydr. Polym.*, 2013, **94**, 749–754.

37 S. L. Williamson, R. Scott Armentrout, R. S. Porter and C. L. McCormick, *Macromolecules*, 1998, **31**, 8134–8141.

38 A. K. Bajpai and A. Mishra, *J. Appl. Polym. Sci.*, 2004, **93**, 2054–2065.

39 A. K. Bajpai and A. Mishra, *Polym. Int.*, 2005, **54**, 1347–1356.

40 M. Pandey, M. C. I. M. Amin, N. Mohamad, N. Ahmad and S. Muda, *Polym.-Plast. Technol. Eng.*, 2013, **52**, 1510–1518.

41 K. Mengel and E. A. Kirkby, *Principles of Plant Nutrition*, Kluwer Academic Publishers, Dordrecht, 5th edn, 2001, p. 362, ISBN 978-94-010-1009-2.

42 S. Jin, Y. Wang, J. He, Y. Yang, X. Yu and G. Yue, *J. Appl. Polym. Sci.*, 2013, **128**, 407–415.

43 L. M. Dobre, A. Stoica-Guzun, M. Stroescu, I. M. Jipa, T. Dobre, M. Ferdes and S. Ciumpiliac, *Chem. Pap.*, 2012, **66**, 144–151.

44 M. J. Ramazani-Harandi, M. J. Zohuriaan-Mehr, A. A. Yousefi, A. Ershad-Langroudi and K. Kabiri, *Polym. Test.*, 2006, **25**, 470–474.

45 A. Lungu, F. X. Perrin, L. Belec, A. Sarbu and M. Teodorescu, *Appl. Clay Sci.*, 2012, **38**, 63–69.

46 E. E. Sileo, P. J. Morando, E. C. Baumgartne and M. A. Blesa, *Thermochim. Acta*, 1991, **184**, 295–303.

47 H. S. Barud, A. M. de Araújo Júnior, D. B. Santos, R. M. N. de Assunção, C. S. Meireles, D. A. Cerqueira, G. R. Filho, C. A. Ribeiro, Y. Messaddeq and S. J. L. Ribeiro, *Thermochim. Acta*, 2008, **471**, 61–69.

48 M. W. Ullaha, M. U. Islama, S. Khana, Y. Kima and J. K. Parka, *Carbohydr. Polym.*, 2016, **136**, 908–916.

49 X. Qi, J. Li, W. Wei, G. Zuo, T. Su, X. Pan, J. Zhang and W. Dong, *RSC Adv.*, 2017, **7**, 14337–14347.

50 A. Mandal and D. Chakrabarty, *Plastics Research Online*, 2015, DOI: 10.2417/spepro.006172.

51 K. J. De France, F. Xu and T. Hoare, *Adv. Healthcare Mater.*, 2017, 1700927–1700944.

52 B. Cheng, B. Pei, Z. Wang and Q. Hu, *RSC Adv.*, 2017, **7**, 42036–42046.

53 E. Trovatti, L. Oliveira, C. S. R. Freire, A. J. D. Silvestre, C. P. Neto, J. J. C. Cruz Pinto and A. Gandini, *Compos. Sci. Technol.*, 2010, **70**, 1148–1153.

54 E. A. James and D. Richards, *Sci. Hortic. (Amsterdam, Neth.)*, 1986, **28**, 201–208.

55 R. S. H. Wong, M. Ashton and K. Dodou, *Pharmaceutics*, 2015, **7**, 305–319.